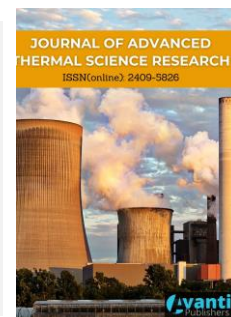




Published by Avanti Publishers  
**Journal of Advanced Thermal  
Science Research**  
ISSN (online): 2409-5826



# Experimental Evaluation and Development of Artificial Neural Network Model for the Solar Stills Augmented with the Permanent Magnet and Sandbag

Rishika Chauhan<sup>1</sup>, Pankaj Dumka<sup>2</sup> and Dhananjay R. Mishra<sup>2,\*</sup>

<sup>1</sup>Department of Electronics and Communication; <sup>2</sup>Department of Mechanical Engineering, Jaypee University of Engineering and Technology, A.B. Road, Guna-473226, Madhya Pradesh (India).

## ARTICLE INFO

*Article Type:* Research Article

*Keywords:*

ANN  
Solar Still  
Desalination  
LM algorithm  
Permanent magnets

*Timeline:*

Received: January 03, 2022

Accepted: March 15, 2022

Published: April 14, 2022

*Citation:* Chauhan R, Dumka P, Mishra DR. Experimental Evaluation and Development of Artificial Neural Network Model for the Solar Stills Augmented with the Permanent Magnet and Sandbag. J Adv Therm Sci Res. 2022; 9: 9-23.

*DOI:* <https://doi.org/10.15377/2409-5826.2022.09.2>

## ABSTRACT

The availability of potable water is reducing day by day due to rapid growth in the human population and un-planned industrialization around the globe. Although human beings cannot think of survival in the absence of water, the global leadership can still not implement their pacts in reality. Solar still is one of the prominent ways of getting potable water from contaminated water. This manuscript reports the experimental evaluation and developed ANN model for the single basin solar stills having augmentations with the sand-filled cotton bags and ferrite ring permanent magnets. Root mean square error (RMSE), efficiency coefficient (E), the overall index of model performance (OI), and coefficient of residual mass (CRM) values are in good agreement with the proposed developed model of ANN. The proposed ANN model can be utilized to predict distillate yield with a variation of 5% for the reported modified stills. Overall correlation coefficient of CSS, MSS-1&2 are 0.98171, 0.9867, and 0.99542, respectively.

\*Corresponding Author

Email: dm30680@gmail.com

Tel: (+91)9893808251

# 1. Introduction

The water crisis is one of the biggest challenges for human beings, and the situation is worsening with every passing year. The exponential population, deforestation, and industrial growth are the major reason for the potable water crisis. Although we are surrounded by two-thirds of water, less than 1% of it is potable. Industries are not only creating air but also water pollution, resulting in a potable water crisis. Researchers nowadays have started thinking in the direction of how to convert salty/brackish water into potable water by adopting sustainable, cost-effective, and environmentally friendly ways. Solar energy is one such perpetual source of energy that meets the entire above criterion. The device which uses solar energy as the input for converting brackish/salty water into potable water is called a conventional solar still (CSS). The device works on the greenhouse principle. The working and construction of CSS are very simple and easy. The major concern is the low productivity and efficiency of this device. So, to enhance the overall performance of CSS, several modifications have been reported by many researchers. Ayoub and Malaeb have reported a detailed review on the novel solar designs still for enhancing their performance [1]. Dumka and Mishra [2] have reported that the optimum solar performance can still be achieved with a salt concentration of 1% due to surface tension and heat capacity break-even at this value. Xiao *et al.* [3] have reported a review on different heat, and mass transfer approaches for the overall understanding of design parameters of solar still. Muftah *et al.* have talked of different ambient, design, and operating parameters that affect the distillate output from a conventional solar still [4]. An extensive review of different design and operating parameters, which still influence the productivity of conventional solar, has been reported by Panchal and Patel [5]. An extensive review of different changes to enhance conventional solar performance has still been reported by Kabeel *et al.* [6]. Dumka and Mishra [7, 8] have reported the use of solar earth stills which utilize ground energy for the performance improvement of solar stills. Kabeel *et al.* [9] have reported the influence of mass and height of the water and its flow rate on the performance of CSS, inclined distiller unit, and CSS integrated with inclined distiller unit. They have observed that the highest distiller yield is obtained for a basin water mass of 6.2 kg for CSS augmented with an inclined distiller unit viz 46.23% more than CSS. To increase the distillate output from a CSS, Zanganeh *et al.* [10] have applied a transparent nano coat solution on the inner side of condensing cover so that the condensing mechanism shifts from film to dropwise. They have reported a distillate increase of 23% higher in the presence of nano coats. Das *et al.* [11] have reviewed the current trends for distillate improvement of CSS. They have focused more on PV and Peltier modules, external condensers, sensible and latent heat-absorbing materials, nanoparticles, humidifiers, and external reflectors. To increase the heat transfer rate within the solar still Mevada *et al.* [12] have reported the use of fin. Moreover, they have also observed that the distillate output is weakly dependent on the fin thickness. Hansen *et al.* have reported an experimental endeavor in which they have used different types of wicks (wood pulp paper, polystyrene sponge, and water coral fleece) and absorber plate (wire mesh, flat, and rectangular stepped) to increase the overall performance of CSS. They have observed that coral wick along with wire mesh gives the highest distillate (viz. 4.28 l/day) in comparison to the other combinations. Saleh *et al.* [13] have reported the performance of solar distiller units augmented with a blend of phase change material and  $\text{Al}_2\text{O}_3$ . An impact of sand-filled glass bottles on the performance improvement of CSS has been reported by Dumka *et al.* [14]. They have reported an increase of 21.32% more distillate output due to the augmentations compared to the CSS. The use of solar power fountains to enhance the surface area of water and, ultimately, the evaporation rate has been reported by Dumka *et al.* [15]. Mahmood and Ansari [16] have reported a novel approach to enhance the performance of solar still by integrating it with a greenhouse. Due to this augmentation, the distiller unit has yielded 4.03–5.20  $\text{m}^3/\text{day}$ .

Predictive and forecasting models give a new dimension to the research and development of novel solar still designs by acting as a pivot upon which future design projects can be built. The outcome of these models will help in giving an initial guess of distillate output before actual experiments can be performed on the site. This will strengthen the planning, design, and execution of actual experiments and save a lot of effort and money. In this regard, different heat and mass transfer based distillate predictive models have been proposed by several researchers. Dunkle [17] was the first to give a semi-empirical model to predict the distillate output from a conventional solar still. But his model is restricted to a mean and operating temperature range of 50 and 17°C, respectively. Based on the indoor simulations, Clark [18] corrected Dunkle's model by giving a new value of the coefficients (C and n), and his model can predict up to a range of 55°C. Kiatsiriroat [19] followed an entirely

different approach to tackle the problem of distillate prediction; instead of going from heat transfer, he modified Spalding's mass transfer theory and gave a new distillate prediction model based on mass transfer. Working on the initial assumptions of Dunkle, Tsilingiris [20, 21] proposed a modified Dunkle model to predict the distillate output. He used the Chilton-Colburn analogy to arrive at the modified model with an operating range of more than 55 °C. The prime drawback of these forecasting techniques is the complex maths involved on the one hand and the requirement of rigorous calculations on the other.

Moreover, the distillate predicted by these models is sometimes unrealistic, as mentioned by Dumka and Mishra [8]. They have shown that Dunkle, Clark, and Spalding's mass transfer theory predicts the distillate output 59.8%, 165.2%, and 50% higher than the experimental results, respectively. Here comes the importance of the Artificial Neural Network (ANN), which is capable of predicting the distillate output from CSS easily, and the results thus obtained are also promising and reliable as compared to other heat transfer based models [22]. The thermodynamic modeling of complex and ill-posed problems is very difficult, but a trained ANN model can easily handle such problems [23, 24]. It doesn't matter much to a robust ANN model that the problem is linear or non-linear; moreover, its prediction speed is very fast. The ANN, its architecture, and its application in the field of renewable energy have been explained in great depth by Kalogirou [25].

Gao *et al.* [23] have proposed an ANN model to model seawater desalination. They have taken the dry and wet bulb temperature of the air, the sprinkler temperature of seawater, and the inlet and outlet cooling water temperature as the input variables and the distillate yield as the output. They have reported a high degree of prediction accuracy of the developed ANN model. A Competition Algorithm-based ANN model to predict the distillate output, exergy efficiency, and energy efficiency of a CSS has been reported by Nazari *et al.* [26]. They have observed that a hidden neuron number of five gives the best performance. Sohani *et al.* [27] have compared the different types of ANN models (Feed-Forward, Radial Basis, and Back Propagation) to predict the hourly yield from a solar distiller unit. They have observed that the ANN model based on a Radial basis gives the best result compared to the others as it shows the highest value of coefficients of determination, viz. 0.977057. With an objective to know the minimum inputs to predict the solar still output (distillate), Santos *et al.* [28] have proposed an ANN model. The model they have reported has been in good agreement with the experimental results. Dumka *et al.* [22] have proposed an ANN model to predict the performance of solar stills augmented with jute-covered plastic balls and compared the results with the experimental data. They have reported that the results are very close to the experimental data with less than 5% error. Chauhan *et al.* [29] have proposed a neural network model to predict the distillate output of solar earth still.

To find the best algorithm for predicting the distillate from a solar still under the influence of a hyper-arid environment, Ahmed *et al.* [30] have performed a comparative study on Resilient backpropagation, Levenberg-Marquardt (LM), and conjugate gradient backpropagation with Fletcher-Reeves restart algorithms. They have reported that out of all the algorithms, the physics of the problem is captured well by the LM algorithm. Mashaly and Alazba [31, 32] have utilized an ANN technique to predict the solar still distillate, which uses agricultural drains as feed water. Hidouri *et al.* [33] have developed an ANN model to predict the distillate output of a novel single slope hybrid solar still integrated with a heat pump (SSDHP). Moreover, they have also provided a way to initially guess the number of hidden layers and neurons to start the ANN simulation. To predict the thermo-physical properties of moist air within the CSS, Chauhan *et al.* [34] have reported an ANN model based on the LM algorithm. They have compared the ANN result with analytical results and have reported that the LM algorithm predicts the properties with a confidence level of more than 95%.

Modified solar still integrated with ferrite ring magnets and sand-filled cotton bags have been reported by Dumka *et al.* [35, 36]. They have observed that the magnets have reduced the surface tension of water and have acted as sensible energy storage pockets, leading to an increase in the distillate output of modified still compared to the conventional solar still. At the same time, the sand-filled cotton bags will enhance the evaporation area and nocturnal distillate output by storing sensible energy. They have used heat and mass transfer models to predict the distillate output of still, but the theoretical results were not very close to the experimental results due to the complex non-linear nature of the problem. The literature has already mentioned that ANN is capable of modeling very complex non-linear problems well. Therefore, the objective of the current research is to design and develop artificial neural network models to predict the distillate output of modified stills augmented with the permanent

ferried ring magnets (16 in number) and sand-filled cotton bags (100 in number) and develop ANN Model based on the LM algorithm is reported in this manuscript.

## 2. Experimental Setup

For experimentation, three identical single basin single slope conventional solar (CSS) were designed and fabricated for the experimental analysis. Fabricated solar stills are made with the help of 5 mm thick fiber reinforced plastic (FRP) material with a 1 m<sup>2</sup> basin area and longer and shorter wall heights of 0.48 and 0.2 m, respectively. For increasing the absorptivity of solar radiations, the stills were painted black from the inside. The condensing cover comprises an iron transparent glass of 4 mm thickness, inclined at an angle of 15.5° with the horizontal. For carrying basin water black painted GI tray is placed in the still. Fig. 1 shows the schematic representation of CSS.

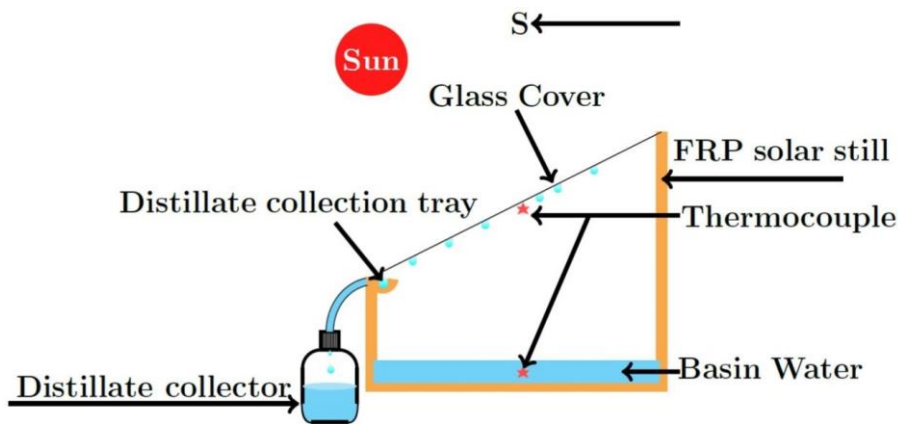


**Figure 1:** Schematic representation of CSS.

One CSS is kept as such, whereas modifications were done in the other two stills. In one of the stills, 100 sand-filled cotton bags were placed of 4 cm internal diameter and 12 cm height each. A total of 20 kg of sand (of 40 GFN) was filled in the bag up to the height of 11 cm, and the remaining 1 cm was filled with charcoal for the better absorption of incident solar radiations. In the manuscript, the still is named as MSS-1 (Modified solar still -1). The schematic of MSS-1 is shown in Fig. 2.

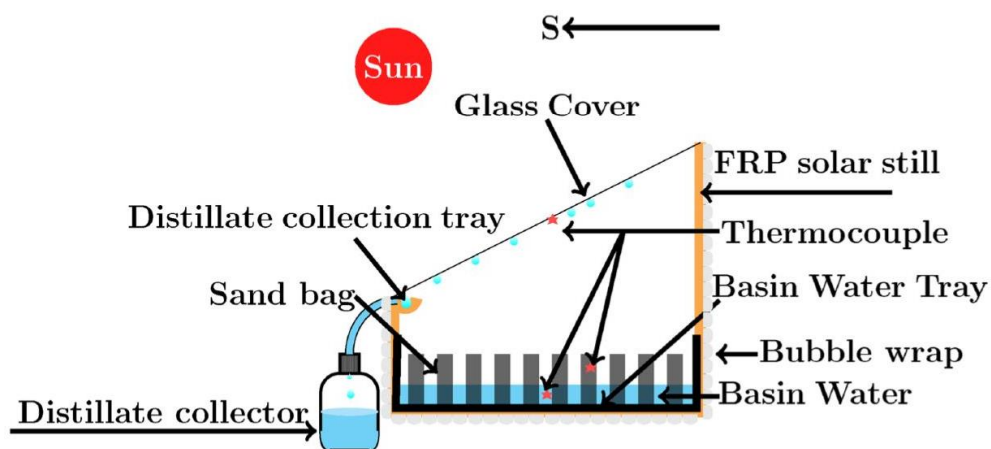


**Figure 2:** Schematic representation of solar still augmented with the sandbag (MSS-1).

In the other CSS, 16 permanent ferrite ring magnets were placed at equal distances, resulting in effective magnetic field strength of 90 mT. The internal diameter, external diameter, and thickness of magnets are 3.2, 6.0, and 0.93 cm, respectively. This still is called MSS-2 (Modified solar still -2) in this manuscript. The schematic of MSS-2 is shown in Fig. 3.

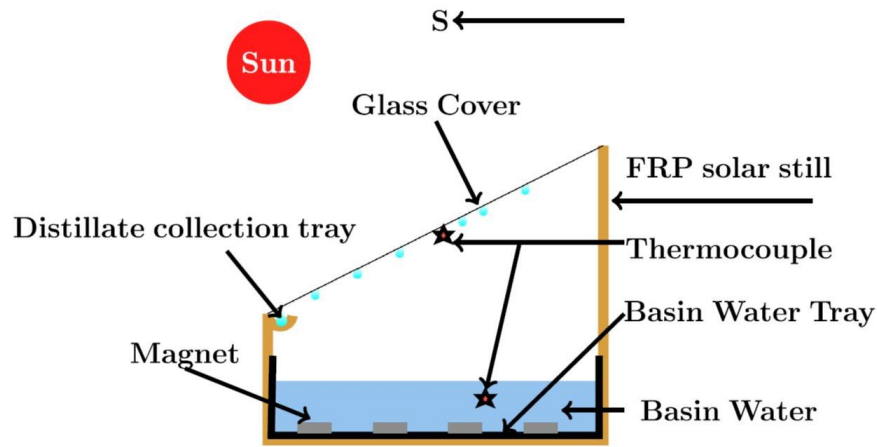


**Figure 3:** Schematic representation of the solar still augmented with the ferrite ring permanent magnet (MSS-2).

The placement and arrangement of sandbags and magnets are shown in Fig. 4a and 4b, respectively. The actual photograph of MSS-1 and MSS-2 is shown in Fig. 5.

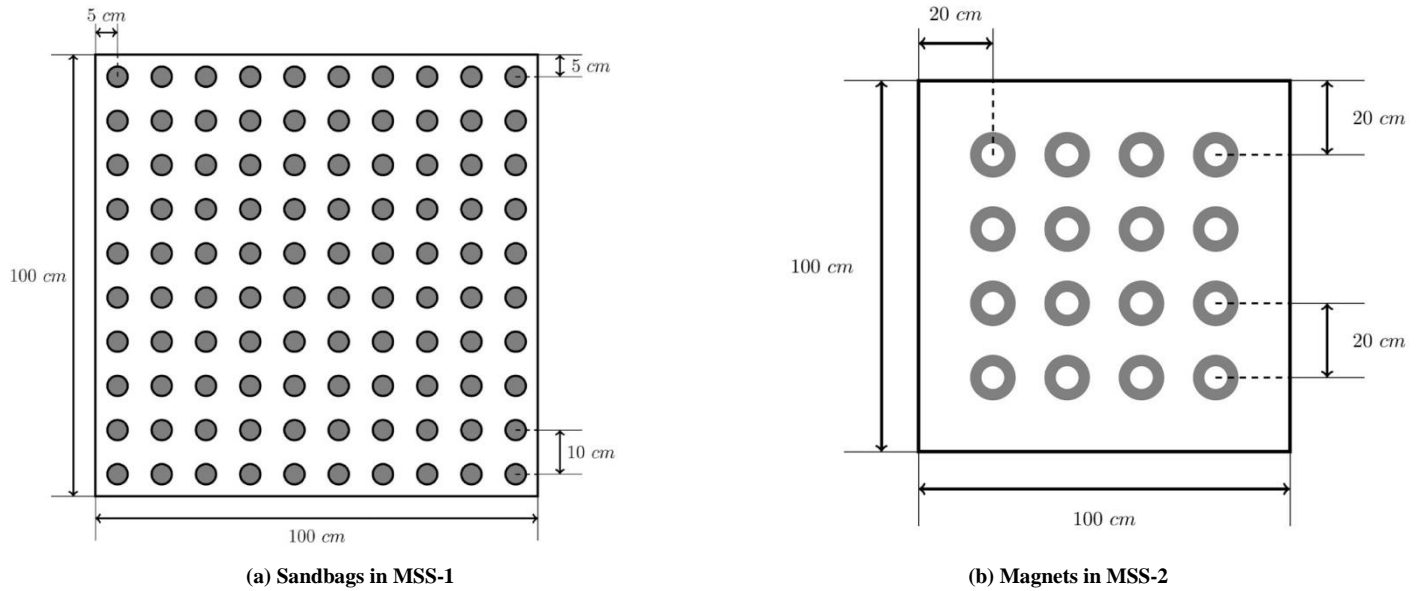


**Figure 4:** Schematic representation of sandbags and magnets within the solar stills.

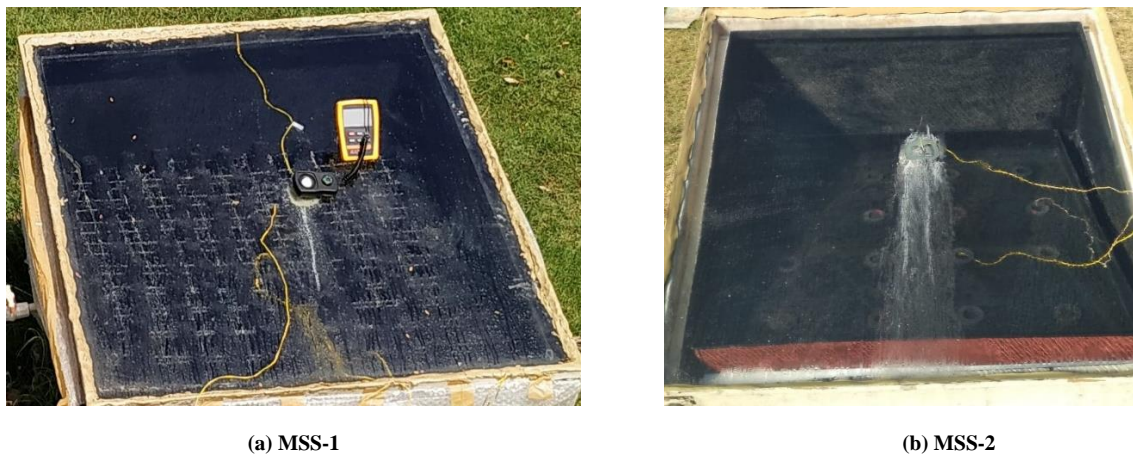


**Figure 5:** Actual photograph of MSS-1 and MSS-2.

For the measurement of different temperatures, K-type thermocouples (K 7/32-2C-TEF) have been used, whereas the DTC324A-2 is used as a temperature indicator. For the measurement of solar radiation intensity, LX-107 has been used. Digital Gaussmeter (OMEGA) has been used to measure magnetic field strength. The distillate output is measured with the help of a Borosil graduated cylinder. The accuracy and range of different types of equipment are tabulated in Table 1. The standard uncertainties are evaluated by considering linear variation in the data, and for that matter, it is considered to be  $a/\sqrt{3}$  where  $a$  is the accuracy of the instrument [37, 38].

**Table 1: Instrument details.**

Instrument	Accuracy	Range	Standard Uncertainties
Solar power meter	$\pm 10 \text{ W/m}^2$	0–2000 $\text{W/m}^2$	5.77 $\text{W/m}^2$
Thermocouple	$\pm 0.1^\circ\text{C}$	–100–500 $^\circ\text{C}$	0.06 $^\circ\text{C}$
Graduated cylinder	$\pm 1 \text{ ml}$	0–250 ml	0.6 ml
Gauss meter	$\pm 1 \text{ G}$	0–2000 G	0.6 G

### 3. ANN Fundamentals

The human brain is the source of inspiration behind neural networks. The idea behind the neural network is to mimic human thinking capability viz. neurons [37] numerically. Like the human brain, the basic element of neural nets is artificial neurons, which may be why they are called artificial neural networks (ANN) [39, 40]. Fig. 6 shows the schematic of an artificial neuron.

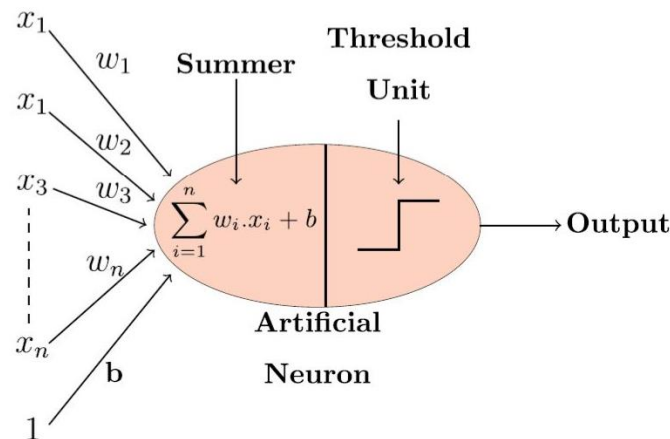


**Figure 6:** Artificial neuron model.

These neurons are interconnected in a network and interact with other neurons through weights and operate in parallel. For neurons to learn, recall, and generalize the data, the fine-tuning of pertinent network parameters is done. It is the responsibility of incoming connections to provide the weighted input signal ( $w_i \times x_i$ ) to the neuron. All the weighted inputs summed ( $\sum w_i \times x_i$ ) are supplied to an activation function, which returns the final output [41]. The activation function used in this article is sigmoid ( $1/(e^{-\text{weighted sum}} + 1)$ ) which returns output in the range of 0 to 1 [42]. The term training is given to the process of adjusting weights according to some stipulated algorithm. Three basic types of learning mechanisms, viz. supervised, unsupervised, and reinforcement, are used to train the network by making subtle network parameter adjustments.

In supervised learning, the desired and network output are compared, and the difference between them is utilized for the network parameter adjustments (viz.  $w$  and  $b$ ). In the case of unsupervised learning, the desired output is unknown, so the parameters are adjusted on the basis of input associations. The environmental feedback is taken in the case of reinforcement learning that's why it is similar to the supervised one. These feedbacks are responsible for the network parameter adjustments.

Feed-forward and feedback are the major classes of ANN. In feed-forward ANN, the network information travels from input to output, i.e., unidirectional. The layer in an ANN model depends on the type of problem, i.e., one (for simple problem) to multi (for complex problem). For  $\alpha$  input nodes, the hidden nodes (M) number in multilayer ANN varies between  $\alpha$  and  $\alpha + 1$  [33].

In this research article, a multilayer perceptron network based on supervised learning has been used, which has been trained by using the Backpropagation (BP) algorithm. BP utilizes gradient/steepest descent for error function minimization. This algorithm minimizes the error by error functions backward propagation for the weights adjustments.

### 3.1. Backpropagation Learning Algorithm Based on Levenberg Marquardt (LM) Algorithm

For obtaining an optimum solution to complex non-linear problems from an ANN model, the Levenberg Marquardt (LM) [43] is one of the popular algorithms. This is called a hybrid algorithm, a blend of steepest descent and Gauss-Newton [44]. The LM algorithm does not require the computation of the Hessian matrix for the updation of weights, and still, it approaches second-order training speed [45]. Hence, it is an efficient method of weight updation. In the LM algorithm, the step size reduces as the iteration increases, i.e., the largest step size in the first iteration (according to gradient descent) and then gradual reduction (according to Gauss-Newton in successive iterations [46].

The Hessian matrix ( $H$ ) and the gradient ( $g$ ) are evaluated as [46]:

$$H = J^T J \quad (1)$$

$$g = J^T e \quad (2)$$

The following update is used to approximate the Hessian matrix by LM algorithm [47, 48]:

$$x_{k+1} = x_k - (J^T J + \mu I)^{-1} J^T e \quad (3)$$

The smaller value of  $\mu$  corresponds to Gauss-Newton, whereas the larger one corresponds to gradient descent. Therefore, LM combines both gradient descent and Gauss-Newton and takes their best part by rejecting their drawbacks.

### 3.2. Performance Evaluation of LM Algorithm

The performance of the LM algorithm is evaluated based on the below-mentioned parameters[30,49,50]:

Root mean square error (RMSE):

$$RMSE = \sqrt{\frac{\sum_{i=1}^N (a_{p,i} - a_{o,i})^2}{N}} \quad (4)$$

Efficiency coefficient (E):

$$E = 1 - \frac{\sum_{i=1}^N (a_{p,i} - a_{o,i})^2}{\sum_{i=1}^N (a_{p,i} - \bar{a}_o)^2} \quad (5)$$

The overall index of model performance (OI):

$$OI = \frac{1}{2} \left( 1 - \frac{RMSE}{a_{max} - a_{min}} + E \right) \quad (6)$$

Coefficient of residual mass (CRM):



$$CRM = \frac{\sum_{i=1}^N a_{p,i} - \sum_{i=1}^N a_{o,i}}{\sum_{i=1}^N a_{o,i}} \quad (7)$$

The RMSE is the efficiency indicator of the ANN model; lower RMSE means better prediction [51]. The perfect fit between observed and predicted is given by OI and E values which are 1.0. Over and underprediction of the model is dictated by the value of CRM (0 means perfect fit).

### 3.3. ANN Model and Methodology Used

In this research, feed-forward BP ANN consists of 3 layers (viz. 1 input, 1 hidden, and 1 output layer) has been used. To train the model LM algorithm has been adopted. The following table depicts the input and output variables for CSS, MSS-1, and MSS-2:

**Table 2: ANN's input and output variables.**

	Input Variable					Output Variable
	$T_w$	$T_{ci}$	$T_a$	$T_{sb}$	$I'$	$\dot{m}_{ew}$
CSS	✓	✓	✓		✓	✓
MSS-1	✓	✓	✓	✓	✓	✓
MSS-2	✓	✓	✓		✓	✓

ANN with (12,1) neuron numbers has been built, and to train, test, and validate the network, MATLAB (R2019) has been used. The schematic of the developed ANN model is shown in Fig. 7.

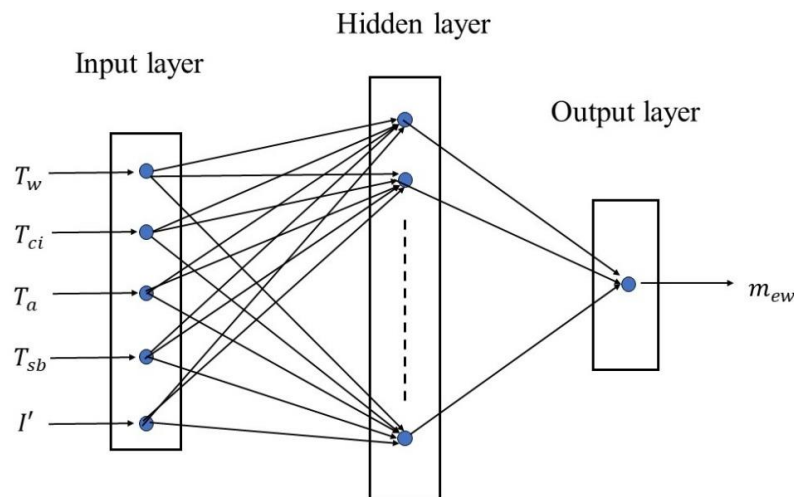


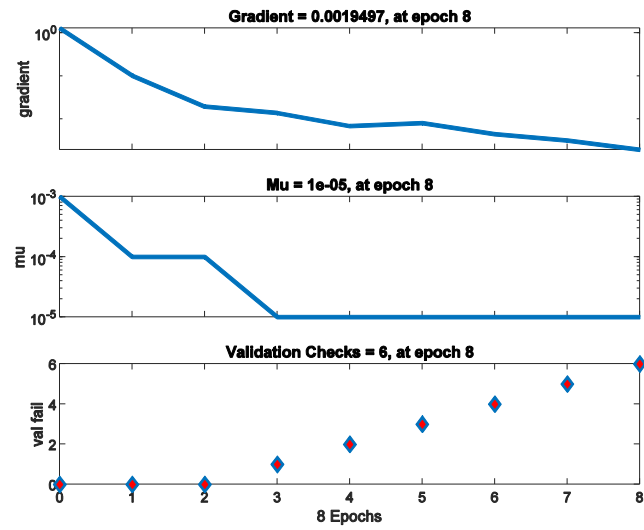
**Figure 7:** Developed ANN model.

## 4. Observations, Results, and Discussions

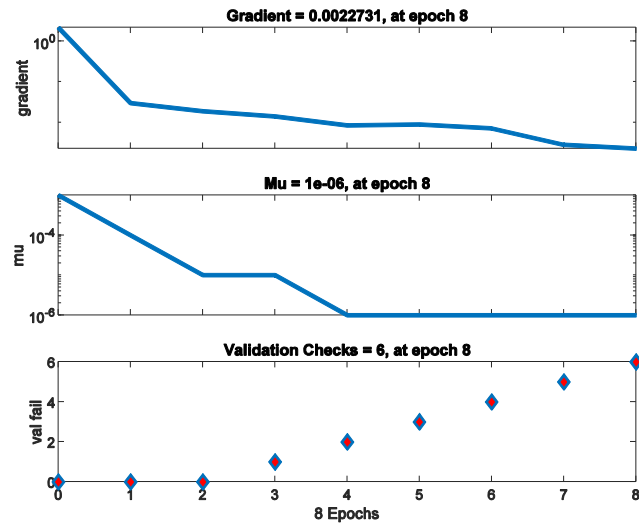
The proposed neural network is trained using the LM algorithm. The variation in gradient error, step size, and validation checks are shown in Fig. 8. The gradient error observed in CSS, MSS-1 and MSS-2 is 0.0019497, 0.0022731, and 0.003229, respectively. At epoch 8, the step size is 1e-05 in CSS and 1e-06 in MSS-1, while the value of  $u$  in MSS-2 is 1e-05 at epoch 11. The validation checks in all three are 6, and the scattered points show increased validation error. With increasing validation error, training stops, and the weights with the lowest error are taken as final weights are shown in Fig. 9.

Fig. 10 shows the mean square error performance observed in CSS, MSS-1, and MSS-2. The best validation performance is noticed at epoch 2 in CSS and MSS-1, and MSS-2 gives the best validation performance at epoch 5.

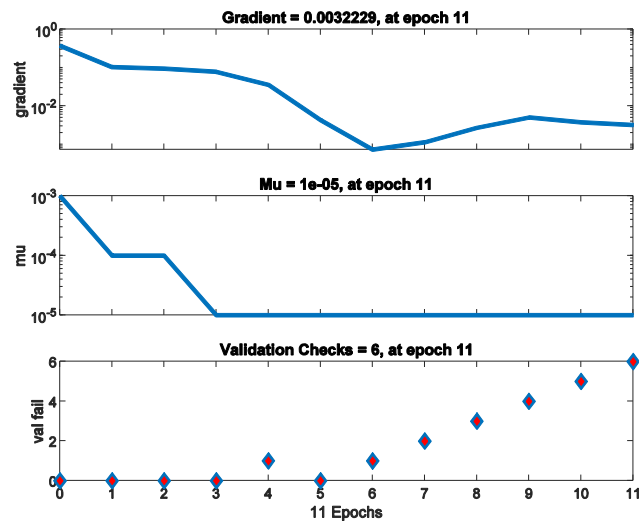




(a) CSS

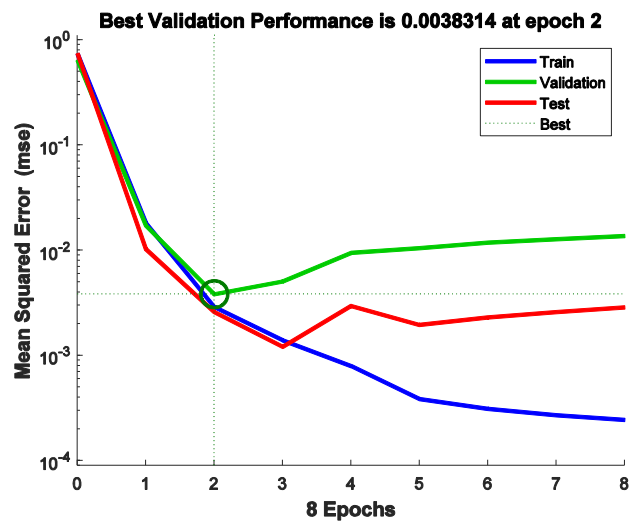


(b) MSS-1

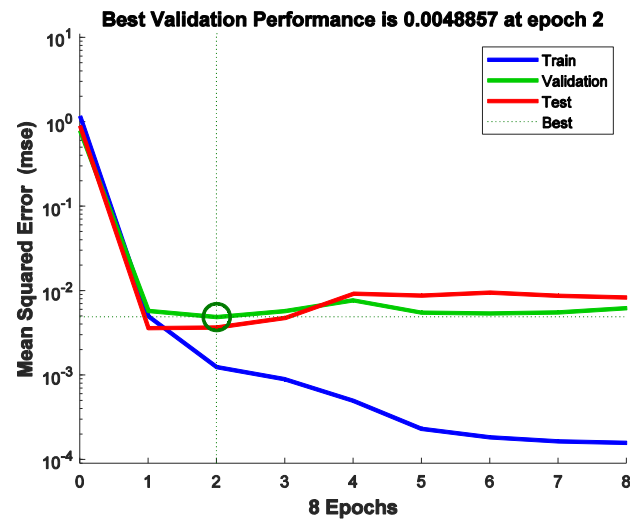


(c) MSS-2

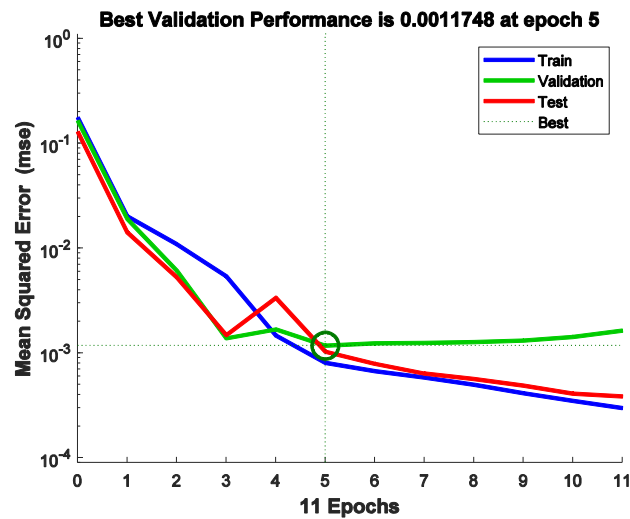
**Figure 8:** Gradient error,  $\mu$ , and validation check variations for CSS, MSS-1, and MSS-2.



(a) CSS



(b) MSS-1



(c) MSS-2

**Figure 9:** MSE Variation for CSS,MSS-1, and MSS-2.

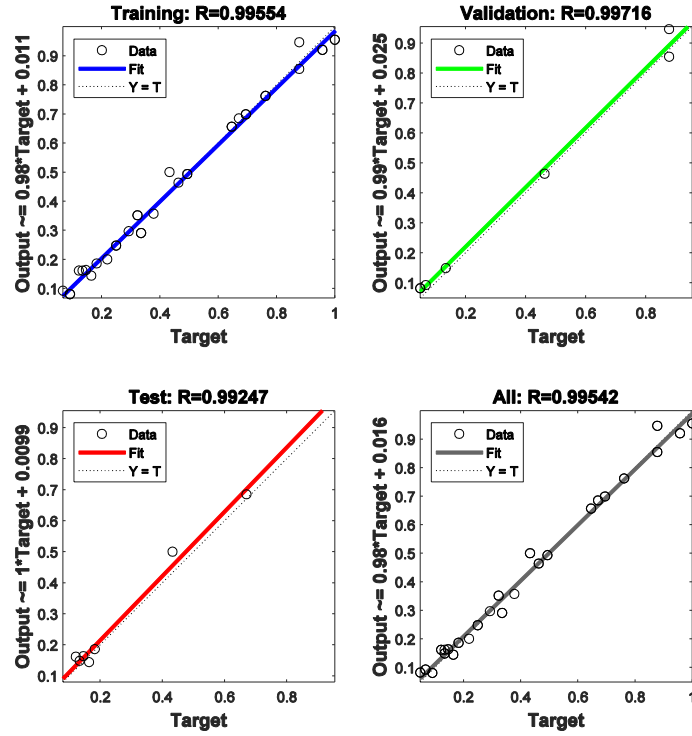
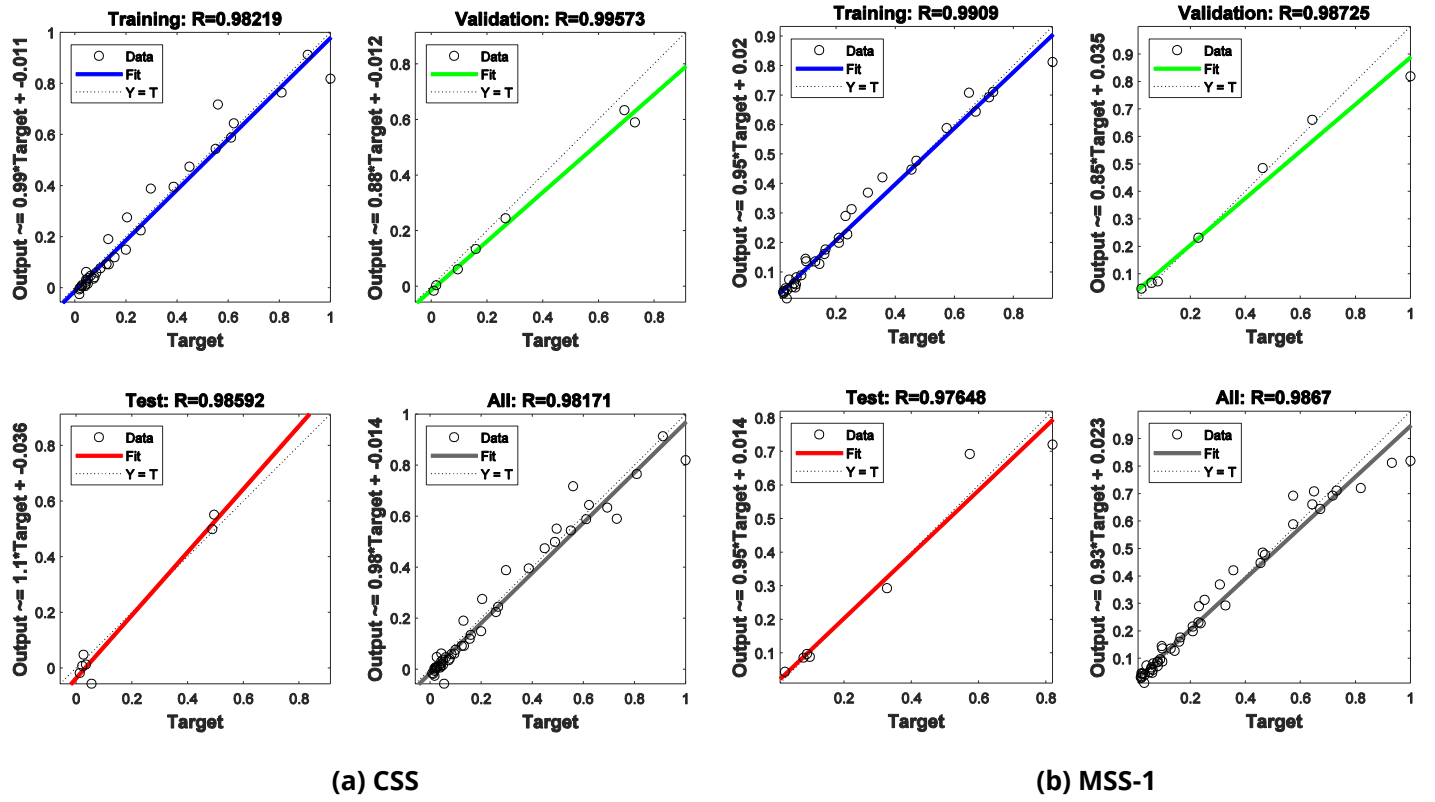


**Figure 10:** Regression analysis using LM algorithm in CSS, MSS-1, and MSS-2.

Regression plots with training, testing, and validation are shown in Fig. 11. The solid line represents the perfect correlation between the predicted and targeted values, and the data points are specified using small circles. The overall value of the correlation coefficient in CSS, MSS-1, and MSS-2 is 0.98171, 0.9867, and 0.99542, respectively. It

is clear that different correlation coefficients clearly reveal the developed model's excellent performance in predicting the targeted values perfectly.

The statistical parameters performance of the LM algorithm for CSS, MSS-1, and MSS-2 are listed in Table 3.

**Table 3: RMSE, E, OI, and CRM values for CSS, MSS-1, and MSS-2.**

	CSS	MSS-1	MSS-2
<b>RMSE</b>	0.0546	0.0462	0.0299
<b>E</b>	0.9591	0.9711	0.9903
<b>OI</b>	0.9520	0.9620	0.9795
<b>CRM</b>	-0.0742	0.0114	0.0131

Comparing the statistical parameters for CSS, MSS-1, and MSS-2, the value of RMSE is low, and the value of E and OI is high for MSS-2. The value of CRM is negative for CSS, which depicts that the curve is under-fitted. The ideal value of CRM is zero, which shows the best fit between predicted and targeted values. From Table 3, it is realized that MSS-2 provides the best performance.

Fig. 11 shows the % error variation for CSS, MSS1, and MSS2 for the proposed ANN model. It has been observed that the proposed model predicts the distillate output of different stills with a confidence level of more than 95%.

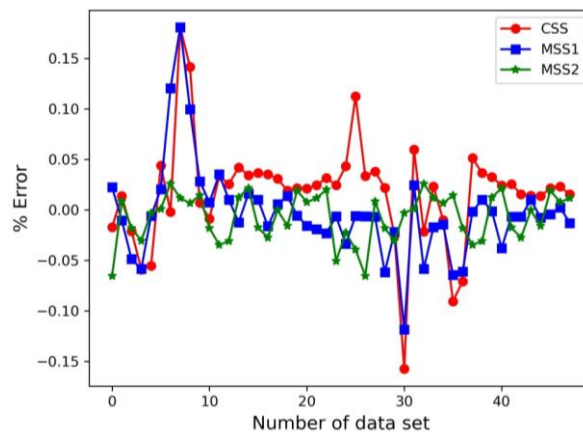


**Figure 11:** Variation of % error of the ANN with respect to the concerned data set.

## 5. Conclusions

Based on the obtained results from the ANN model and experimental data following conclusions can be drawn:

- Once knowing the input parameters, one can quickly obtain the performance of CSS, MSS-1, and MSS-2 by applying the proposed ANN model.
- The proposed ANN model is giving promising results based on obtained RMSE, E, OI, R<sup>2</sup>, and CRM values for CSS, MSS-1, and MSS-2.
- The predicted distillate from CSS, MSS-1, and MSS-2 has less than 5% variation compared to the experimental data.
- The developed ANN model based on the LM algorithm will be helpful in forecasting distillate from new solar still plants integrated with sandbags and magnets, as it eliminates the requirement of solving complex heat and mass transfer equations.

## Nomenclatures

$a_{p,i}$	Predicted value
$a_{o,i}$	Observed value
$\bar{a}_o$	Average observed value
$a_{max}$	Maximum observed value
$a_{min}$	Minimum observed value
$b$	Bias
$e$	Network error vector
$E$	Efficiency coefficient
$g$	Gradient
$H$	Hessian matrix
$I(t)$	Incident solar radiation on inclined cover surface (W/m <sup>2</sup> )
$I'$	Identity matrix
$J$	Jacobian matrix
$J^T$	Transpose of Jacobian matrix
$m_{ew}$	Distillate output (ml)
$N$	No of samples
$R$	Correlation coefficient
$R^2$	Coefficient of determination
$T_a$	Ambient temperature (°C)
$T_{ci}$	Inner glass cover temperature (°C)
$T_{sb}$	Sand bag temperature (°C)
$T_w$	Temperature of water surface (°C)
$w_i$	Weight
$x_i$	Input variable

### Greek Letter

$\mu$	Damping factor
-------	----------------

### Abbreviations

ANN	Artificial neural network
CRM	Coefficient of residual mass
CSS	Conventional solar still
FRP	Fiber reinforced plastic
LM	Levenberg Marquardt
MSSIE	Modified solar still integrated with sand bed earth
OI	Overall index of model performance
RMSE	Root mean square error

## References

- [1] Ayoub GM, Malaeb L. Developments in solar still desalination systems: A critical review. *Crit Rev Environ Sci Technol.*, 2012; 42(19): pp. 2078-2112. <https://doi.org/10.1080/10643389.2011.574104>
- [2] 2] Dumka P, Mishra DR. Influence of salt concentration on the performance characteristics of passive solar still. *Int J Ambient Energy*, 2019. <https://doi.org/10.1080/01430750.2019.1611638>
- [3] Xiao G, *et al.* A review on solar stills for brine desalination. *Appl Energy*, 2013; 103: pp. 642-652. <https://doi.org/10.1016/j.apenergy.2012.10.029>
- [4] Muftah AF, Alghoul MA, Fudholi A, Abdul-Majeed MM, Sopian K. Factors affecting basin type solar still productivity: A detailed review. *Renew Sustain Energy Rev*, 2014; 32: pp. 430-447. <https://doi.org/10.1016/j.rser.2013.12.052>
- [5] Panchal HN, Patel S. An extensive review on different design and climatic parameters to increase distillate output of solar still. *Renew Sustain Energy Rev*, 2017; 69(December 2015): pp. 750-758, Mar. <https://doi.org/10.1016/j.rser.2016.09.001>
- [6] Kabeel AE, Manokar AM, Sathyamurthy R, Winston DP, El-Agouz SA, Chamkha AJ. A Review on Different Design Modifications Employed in Inclined Solar Still for Enhancing the Productivity. *J Sol Energy Eng*, 2018; 141(3): p. 031007. <https://doi.org/10.1115/1.4041547>
- [7] Dumka P, Mishra DR. Energy and exergy analysis of conventional and modified solar still integrated with sand bed earth: Study of heat and mass transfer. *Desalination*, 2018; 437(July 2018): pp. 15-25. <https://doi.org/10.1016/j.desal.2018.02.026>
- [8] Dumka P, Mishra DR. Experimental investigation of modified single slope solar still integrated with earth (I) &(II):Energy and exergy analysis. *Energy*, 2018; 160: pp. 1144-1157, Oct. <https://doi.org/10.1016/j.energy.2018.07.083>
- [9] 9] Kabeel AE, Taamneh Y, Sathyamurthy R, Kumar PN, Manokar AM, Arunkumar T. Experimental study on conventional solar still integrated with inclined solar still under different water depth. *Heat Transf - Asian Res*, 2019; 48(1): pp. 100-114. <https://doi.org/10.1002/htj.21370>
- [10] Zanganeh P, *et al.* Productivity enhancement of solar stills by nano-coating of condensing surface. *Desalination*, 2019; 454(December 2018): pp. 1-9. <https://doi.org/10.1016/j.desal.2018.12.007>
- [11] Das D, Bordoloi U, Kalita P, Boehm RF, Kamble AD. Solar still distillate enhancement techniques and recent developments. *Groundw Sustain Dev*, 2020; 10(March): p. 100360. <https://doi.org/10.1016/j.gsd.2020.100360>
- [12] Mevada D, *et al.* Effect of fin configuration parameters on performance of solar still: A review. *Groundw Sustain Dev*, 2020; 10(September 2019): p. 100289. <https://doi.org/10.1016/j.gsd.2019.100289>
- [13] Saleh B, *et al.* Investigating the performance of dish solar distiller with phase change material mixed with Al<sub>2</sub>O<sub>3</sub> nanoparticles under different water depths. *Environ Sci Pollut Res*, 2022. <https://doi.org/10.1007/s11356-021-18295-4>
- [14] Dumka P, Gautam H, Sharma S, Gunawat C, Mishra DR. Impact of Sand Filled Glass Bottles on Performance of Conventional Solar Still. *J Basic Appl Sci*, 2022; 18: pp. 8-15. <https://doi.org/10.29169/1927-5129.2022.18.02>
- [15] Dumka P, Sharma S, Gautam H, Gunawat C. Impact of Solar Powered Fountain on The Performance of Conventional Solar Still. *Int J Eng Res Technol*, 2021; 10(11): pp. 109-112.
- [16] Mahmood F, Al-Ansari T. Design and analysis of a renewable energy driven greenhouse integrated with a solar still for arid climates. *Energy Convers Manag*, 2022; 258: p. 115512. <https://doi.org/10.1016/j.enconman.2022.115512>
- [17] Dunkle RV. Solar water distillation: the roof type still and a multiple effect diffusion still. in *International Developments in Heat Transfer*, ASME, Proc International Heat Transfer, Part V, University of Colorado, 1961, pp. 895-902.
- [18] Clark JA. The steady-state performance of a solar still. *Sol Energy*, 1990; 44(1): pp. 43-49. [https://doi.org/10.1016/0038-092X\(90\)90025-8](https://doi.org/10.1016/0038-092X(90)90025-8)
- [19] Kiatsirirot T, Bhattacharya SC, Wibulswas P. Prediction of mass transfer rates in solar stills. *Energy*, 1986; 11(9): pp. 881-886, Sep. [https://doi.org/10.1016/0360-5442\(86\)90007-1](https://doi.org/10.1016/0360-5442(86)90007-1)
- [20] Tsilingiris PT. Combined heat and mass transfer analyses in solar distillation systems - The restrictive conditions and a validity range investigation. *Sol Energy*, 2012; 86(11): pp. 3288-3300. <https://doi.org/10.1016/j.solener.2012.08.009>
- [21] Tsilingiris PT. Parameters affecting the accuracy of Dunkle ' s model of mass transfer phenomenon at elevated temperatures. *Appl Therm Eng*, 2015; 75: pp. 203-212. <https://doi.org/10.1016/j.applthermaleng.2014.09.010>
- [22] Dumka P, Chauhan R, Mishra DR. Experimental and theoretical evaluation of a conventional solar still augmented with jute covered plastic balls. *J Energy Storage*, 2020; 32(June): p. 101874. <https://doi.org/10.1016/j.est.2020.101874>
- [23] Kalogirou SA, Mathioulakis E, Belessiotis V. Arti fi cial neural networks for the performance prediction of large solar systems. *Renew Energy*, 2014; 63: pp. 90-97. <https://doi.org/10.1016/j.renene.2013.08.049>
- [24] Essa FA, Abd Elaziz M, Elsheikh AH. An enhanced productivity prediction model of active solar still using artificial neural network and Harris Hawks optimizer. *Appl Therm Eng*, 2020; 170(August 2019): p. 115020. <https://doi.org/10.1016/j.applthermaleng.2020.115020>
- [25] Kalogirou SA, Panteliou S, Dentsoras A. Artificial neural networks in renewable energy systems applications: a review. *Renew Sustain Energy Rev*, 2001; 5(4): pp. 373-401. [https://doi.org/10.1016/S1364-0321\(01\)00006-5](https://doi.org/10.1016/S1364-0321(01)00006-5)
- [26] Nazari S, Bahraei M, Moayedi H, Safarzadeh H. A proper model to predict energy efficiency, exergy efficiency, and water productivity of a solar still via optimized neural network. *J Clean Prod*, 2020; 277: p. 123232. <https://doi.org/10.1016/j.jclepro.2020.123232>

- [27] Sohani A, Hoseinzadeh S, Samiezadeh S, Verhaert I. Machine learning prediction approach for dynamic performance modeling of an enhanced solar still desalination system. *J Therm Anal Calorim*, 2022; 147(5): pp. 3919-3930. <https://doi.org/10.1007/s10973-021-10744-z>
- [28] Santos NI, Said AM, James DE, Venkatesh NH. Modeling solar still production using local weather data and artificial neural networks. *Renew Energy*, 2012; 40(1): pp. 71-79. <https://doi.org/10.1016/j.renene.2011.09.018>
- [29] Chauhan R, Dumka P, Mishra DR. Modelling conventional and solar earth still by using the LM algorithm-based artificial neural network. *Int J Ambient Energy*, 2020; pp. 1-8. <https://doi.org/10.1080/01430750.2019.1707113>
- [30] Mashaly AF, Alazba AA. Comparative investigation of artificial neural network learning algorithms for modeling solar still production. *J Water Reuse Desalin*, 2015; 5(4): pp. 480-493. <https://doi.org/10.2166/wrd.2015.009>
- [31] Mashaly AF, Alazba AA. Comparison of ANN, MVR, and SWR models for computing thermal efficiency of a solar still. *Int J Green Energy*, 2016; 13(10): pp. 1016-1025. <https://doi.org/10.1080/15435075.2016.1206000>
- [32] Mashaly AF, Alazba AA. Thermal performance analysis of an inclined passive solar still using agricultural drainage water and artificial neural network in arid climate. *Sol Energy*, 2017; 153: pp. 383-395. <https://doi.org/10.1016/j.solener.2017.05.083>
- [33] Hidouri K, Mishra DR, Benhmide A, Chouachi B. Experimental and theoretical evaluation of a hybrid solar still integrated with an air compressor using ANN. *Desalin Water Treat*, 2017; 88(June 2018): pp. 52-59. <https://doi.org/10.5004/dwt.2017.21333>
- [34] Chauhan R, Sharma S, Pachauri R, Dumka P, Mishra DR. Experimental and theoretical evaluation of thermophysical properties for moist air within solar still by using different algorithms of artificial neural network. *J Energy Storage*, 2020; 30(February): p. 101408. <https://doi.org/10.1016/j.est.2020.101408>
- [35] Dumka P, Kushwah Y, Sharma A, Mishra DR. Comparative analysis and experimental evaluation of single slope solar still augmented with permanent magnets and conventional solar still. *Desalination*, 2019; 459. <https://doi.org/10.1016/j.desal.2019.02.012>
- [36] Dumka P, Sharma A, Kushwah Y, Raghav AS, Mishra DR. Performance evaluation of single slope solar still augmented with sand-filled cotton bags. *J Energy Storage*, 2019; 25: p. 100888, Oct. <https://doi.org/10.1016/j.est.2019.100888>
- [37] Dumka P, Mishra DR. Performance evaluation of single slope solar still augmented with the ultrasonic fogger. *Energy*, 2020; 190: p. 116398, Oct. <https://doi.org/10.1016/j.energy.2019.116398>
- [38] Essa FA, Abdullah AS, Omara ZM, Kabeel AE, Gamiel Y. Experimental study on the performance of trays solar still with cracks and reflectors. *Appl Therm Eng*, 2021; 188: p. 116652. <https://doi.org/10.1016/j.applthermaleng.2021.116652>
- [39] Tang S, Yang Y. Why neural networks apply to scientific computing?. *Theor Appl Mech Lett*, 2021; 11(3): p. 100242. <https://doi.org/10.1016/j.taml.2021.100242>
- [40] Katal A, Singh N. Artificial Neural Network: Models, Applications, and Challenges. in *Innovative Trends in Computational Intelligence*, R. Tomar, M. D. Hina, R. Zitouni, and A. Ramdane-Cherif, Eds. Cham: Springer International Publishing, 2022; pp. 235-257. [https://doi.org/10.1007/978-3-030-78284-9\\_11](https://doi.org/10.1007/978-3-030-78284-9_11)
- [41] Jawad J, Hawari AH, Zaidi SJ. Artificial neural network modeling of wastewater treatment and desalination using membrane processes: A review. *Chem Eng J*, 2021; 419: p. 129540. <https://doi.org/10.1016/j.cej.2021.129540>
- [42] Dombi J, Jónás T. The generalized sigmoid function and its connection with logical operators. *Int J Approx Reason*, 2022; 143: pp. 121-138. <https://doi.org/10.1016/j.ijar.2022.01.006>
- [43] Bilski J, Kowalczyk B, Marchlewska A, Zurada JM. Local Levenberg-Marquardt Algorithm for Learning Feedforward Neural Networks. *J Artif Intell Soft Comput Res*, 2020; 10(4): pp. 299-316. <https://doi.org/10.2478/jaiscr-2020-0020>
- [44] Zare H, Hajarian M. An efficient Gauss-Newton algorithm for solving regularized total least squares problems. *Numer Algorithms*, 2022; 89(3): pp. 1049-1073. <https://doi.org/10.1007/s11075-021-01145-2>
- [45] Ozyildirim BM, Kiran M. Levenberg-Marquardt multi-classification using hinge loss function. *Neural Networks*, 2021; 143: pp. 564-571. <https://doi.org/10.1016/j.neunet.2021.07.010>
- [46] Hagan MT, Demuth HB, Beale MH. *Neural Network Design*, 2nd ed. CENGAGE Learning, 1995.
- [47] Meng H, Yuan F, Yan T, Zeng M. Indoor Positioning of RBF Neural Network Based on Improved Fast Clustering Algorithm Combined with LM Algorithm. *IEEE Access*, 2019; 7: pp. 5932-5945. <https://doi.org/10.1109/ACCESS.2018.2888616>
- [48] Gao J, Zhang Y, Du Y, Li Q. Optimization of the tire ice traction using combined Levenberg-Marquardt (LM) algorithm and neural network. *J Brazilian Soc Mech Sci Eng*, 2019; 41(1): p. 40. <https://doi.org/10.1007/s40430-018-1545-2>
- [49] Arbat G, Puig-Bargués J, Barragán J, Bonany J, de Cartagena FR. Monitoring soil water status for micro-irrigation management versus modelling approach. *Biosyst Eng*, 2008; 100(2): pp. 286-296. <https://doi.org/10.1016/j.biosystemseng.2008.02.008>
- [50] Alazba AA, Mattar MA, ElNesr MN, Amin MT. Field assessment of friction head loss and friction correction factor equations. *J Irrig Drain Eng*, 2011; 138(2): pp. 166-176. [https://doi.org/10.1061/\(ASCE\)IR.1943-4774.0000387](https://doi.org/10.1061/(ASCE)IR.1943-4774.0000387)
- [51] Jalal FE, Xu Y, Iqbal M, Javed MF, Jamhiri B. Predictive modeling of swell-strength of expansive soils using artificial intelligence approaches: ANN, ANFIS and GEP. *J Environ Manage*, 2021; 289: p. 112420. <https://doi.org/10.1016/j.jenvman.2021.112420>